Environmental Science
Processes & Impacts

Uptake and release of perfluoroalkyl carboxylic acids (PFCAs) from macro and microplastics

Journal:	*Environmental Science: Processes & Impacts*
Manuscript ID	EM-ART-05-2023-000209.R2
Article Type:	Paper

Environmental significance: This lab-based study has vital implications for the environmental fate and behavior of microplastics and PFAS. The study uncovers the interactions between PFCAs (a prevalent subclass of PFAS) and microplastics, revealing their potential to mutually influence their properties in aquatic environments. The adsorption of PFCAs onto microplastics, driven by hydrophobic interactions, highlights microplastics' role as vectors for PFCA transport. Sunlight-induced weathering triggers PFCA desorption, with chain length playing a crucial role in this process. These findings emphasize the need to consider the joint occurrence of microplastics and PFCAs in the environment, especially in areas impacted by aqueous firefighting foam (AFFF). Understanding these interactions is essential for developing effective strategies to tackle the environmental risks associated with these emerging contaminants.

Uptake and release of perfluoroalkyl carboxylic acids (PFCAs) from macro and microplastics

Philip J. Brahana[1], Ahmed Al Harraq[1,‡], Luis E. Saab[1], Ruby Roberg[1], Kaillat T. Valsaraj[1], Bhuvnesh Bharti[1,*]

[1]Cain Department of Chemical Engineering, Louisiana State University, Baton Rouge, Louisiana, 70803 United States

‡*Present address:* Center for the Physics of Biological Function, Princeton University, Princeton, NJ 08544, USA

*Corresponding author. Email: bbharti@lsu.edu

Abstract

Microplastics and per- and polyfluoroalkyl substances (PFAS) are two of the most notable emerging contaminants reported in the environment. Micron and nanoscale plastics possess a high surface area-to-volume ratio, which could increase their potential to adsorb pollutants such as PFAS. One of the most concerning sub-classes of PFAS are the perfluoroalkyl carboxylic acids (PFCAs). PFCAs are often studied in the same context as other environmental contaminants, but their amphiphilic properties are often overlooked in determining their fate in the environment. This lack of consideration has resulted in a diminished understanding of the environmental mobility of PFCAs, as well as their interactions with environmental media. Here, we investigate the interaction of PFCAs with polyethylene microplastics, and identify the role of environmental weathering in modifying the nature of interactions. Through a series of adsorption-desorption experiments, we delineate the role of the fluoroalkyl tail in the binding of PFCAs to microplastics. As the number of carbon atoms in the fluoroalkyl chain increases, there is a corresponding increase in the adsorption of PFCAs onto microplastics. This relationship can become modified by environmental weathering, where the PFCAs are released from the macro and microplastic surface after exposure to simulated sunlight. This study identifies the fundamental relationship between PFCAs and plastic pollutants, where they can mutually impact their thermodynamic and transport properties.

Keywords: Microplastic, PFAS, PFCA, Adsorption, Weathering

1. Introduction

Over the past century, single-use plastics have become a part of everyday life and their use continues to increase globally. Today, legacy plastics persist in the environment, as they populate an overwhelming portion of water on our planet[1–3]. Left in the environment, these plastics can fracture and disintegrate under stress leading to the formation of microplastics (MPs). MPs are defined as sub-cm fragments of plastics which have been deposited in the environment as a result of industrial and consumer waste. As these plastic fragments decrease in size, their surface area-to-volume ratio increases[4], which enhances their potential to adsorb various chemicals including environmental pollutants[3,5–7]. While the presence of MPs in the environment is well-documented,

their impact on human health is currently under debate[8]. Regardless of the potential toxicity of pristine MPs, the adsorption of chemical pollutants on the surface of MPs could render them harmful to living organisms. Therefore, it is critical to understand and analyze the ability of MPs to uptake and release common environmental pollutants.

Similar to MPs, per- and polyfluoroalkyl substances (PFAS) are a relatively new class of synthetic pollutants which are commonly released into the environment. Several PFAS belong to the family of persistent organic pollutants (POPs) and are referred to as "forever chemicals" due to their unmatched stability in a wide range of environmental conditions, coupled with their extremely slow degradation kinetics[9]. One sub-class of PFAS widely used in industry is the perfluoroalkyl carboxylic acids[10], referred to as PFCAs from here on. The PFCAs contain a hydrophobic fluoroalkyl tail which is tuned in length based on the desired application or local regulations. PFCAs have been reported in all types of environments, including freshwater[11], arctic ecosystems[12] and atmospheric water[13] (fog, dew, rain) while also contaminating drinking water throughout the United States[14]. This is particularly alarming due to their potentially carcinogenic effects[15], adverse impacts on brain function[16] and epidemiological association with various illnesses[17]. Existing literature reports the coexistence of MPs and PFCAs in lakes[18] and products from wastewater treatment, such as biosolids or sewage sludge[19,20]. In some instances, biosolids and sewage sludge are utilized as fertilizer in agriculture, leading to the unintentional deposition of these contaminants into the environment via runoff[21] and atmospheric transport[20]. The potential for co-existence of PFCAs and MPs in numerous environments has prompted the development of predictive models to estimate their relationship in different aqueous settings[22]. However, the experimental literature on the mutual interaction between PFAS and MPs, along with the corresponding impact is limited. In a recent field study, PFAS was found to be concentrated on microplastics more abundantly when organic matter was present, however the mechanism of the accumulation of the PFAS on MPs remains unclear[18]. In another study, a predictive model was used to interrogate the complexity of PFCA-MP interactions, where it was demonstrated that the hydrophobicity of the PFCAs is a significant contributor to the adsorption of PFCAs by MPs[22]. However, experimental validation of such predictions is needed to ensure the accuracy and applicability of the models to the real-world scenarios. Currently, we lack the understanding of potential synergetic effects occurring between the two emerging pollutants, which could potentially amplify their threats to the environment and human health. Hence, it is critical to investigate the factors governing the interactions between PFCAs and MPs and thus understand the corresponding changes in the properties of the two pollutants.

In this article, we study the interactions between PFCAs and MPs using adsorption-desorption isotherms. In the real environment, it has been reported that PFCAs can adsorb onto many different surfaces[23], including MPs[18,24], however the fundamental intricacies of this relationship have yet to be elucidated. We use polyethylene (PE) as a model MP and a set of PFCAs with tail lengths ranging from 7-10 C-atoms as model PFCAs. By varying the tail length, we seek to identify the role of the hydrophobic fluoroalkyl tail of the PFCA on their adsorption-desorption from the surface of MPs. We find that PFCAs are readily adsorbed onto the MPs and impact their dispersed state in water. We also investigate the role of sunlight-induced weathering of MPs and common macroplastics on the adsorption capacity and release of the preabsorbed PFCAs into bulk water,

which has potential implications in modeling the environmental transport of PFCAs and MPs. With increasing anthropogenic waste in our oceans, it is necessary to identify how the presence of one pollutant impacts the other. Our study points to the existence of complex relationship between PFCAs and MPs, where both the pollutants mutually impact their thermodynamic and transport properties.

2. Experimental

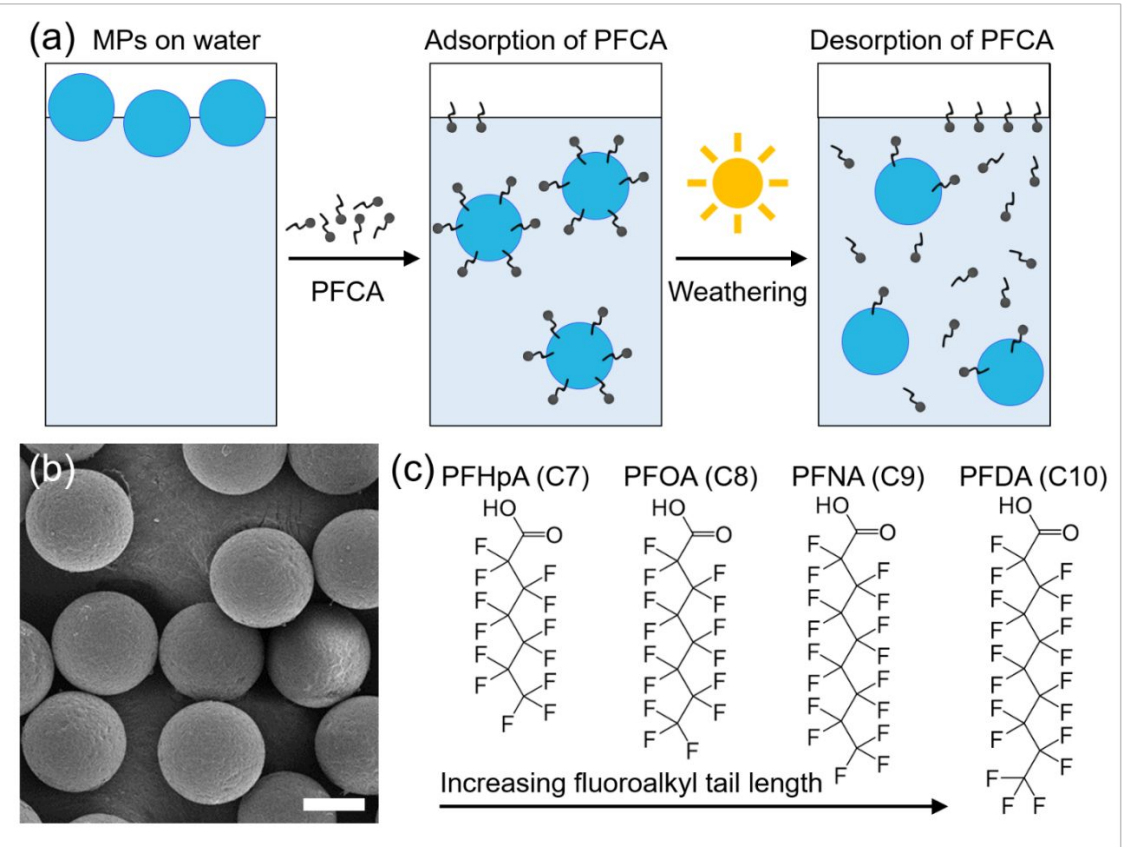

Figure 1: Experimental design. (a) Schematic representation of the experimental process where PFCAs adsorb onto the pristine PE MPs, then sunlight-induced weathering drives the photooxidation of MPs, followed by the subsequent desorption of PFCA molecules. The PFCA molecules and MPs shown in the schematic are not drawn to scale. (b) Scanning electron micrograph of the model PE MPs used in the study. Scale bar = 50 µm. (c) Chemical structures of the four model PFCAs used to investigate the role of fluoroalkyl tail length on their ability to adsorb/desorb from MP surface.

Microplastics are classified as primary and secondary. The primary microplastics are introduced in the environment in their microscopic form, whereas the secondary microplastics are generated in the environment due to the gradual weathering of larger plastic materials[4]. Here we use hydrophobic PE microplastics as a model for primary microplastics. We identify the nature of interactions and corresponding adsorption-desorption relationship between PFCAs and PE MPs in the environment (Fig 1a). PE was chosen as a model MP, as it is estimated to compose nearly half of all plastic waste in the marine ecosystem[25]. Note that such well-defined model MPs were

necessary to clearly understand their interactions with PFCAs, which cannot be achieved with commodity plastics.

The existence of PFAS in the environment is well-documented and includes compounds such as fluorinated polymers, fluorotelomers and perfluoroalkyl acids[26]. We study four model PFCAs with an identical carboxylic acid headgroup and increasing number of C-atoms in the tail. PFCAs have higher interfacial activity relative to their hydrocarbon surfactant counterparts. These characteristics can be attributed to strongly hydrophobic nature of the fluoroalkyl tail, which renders the PFCAs highly active towards hydrophobic interfaces, including air[27]. To better understand the role of the fluoroalkyl chains on the interactions between PFCAs and MPs, we selected four model PFCAs. These PFCAs were chosen as models because of the following three reasons: (1) the potential threat they pose to human health[15,17], (2) their well-documented presence in the environment, both as direct compounds and as products of degradation[28–31] and (3) the systematic variation in fluoroalkyl tail length, which impacts their phase behavior[32] and would provide insights into the underlying interactions between PFCAs and MPs. We test the tail-length dependence of the binding affinity of PFCAs onto the model PE MPs. To do this, we measure the adsorption isotherms of PFCAs on PE MPs in deionized (DI) water at 25°C, where the MPs are nearly neutral and the electrostatic interaction between the PE surface and PFCAs is negligible (discussed in section 3.1).

2.1 Materials

Neutrally buoyant polyethylene microspheres of diameter ~70 μm with a specific surface area of ~0.3 m^2 g^{-1} (Fig. S1 and S2) were purchased from Cospheric LLC (Fig. 1b). The PE MPs were dyed blue in color by the manufacturer, for clarity of visualization during the experiments. The model PFCAs were purchased from Sigma-Aldrich (95% purity) and included perfluoroheptanoic acid (PFHpA - C7), perfluorooctanoic acid (PFOA - C8), perfluorononanoic acid (PFNA - C9) and perfluorodecanoic acid (PFDA - C10) (Fig. 1c).

2.2 Optical tensiometry

The concentration of the model PFCAs in DI water was determined using pendant drop tensiometry performed on an optical tensiometer (Biolin Scientific) and corresponding pendant droplet shape analysis[33–36]. Optical tensiometry and pendant drop analysis is a traditional method to determine surfactant concentrations in water. Pendant drop analysis involves suspending a drop of the liquid phase from the tip of a needle or capillary tube. The pendant drop shape is strongly influenced by the interfacial tension (in addition to gravity), which, in turn, is affected by the surfactant concentration. By analyzing the droplet's contour using Young-Laplace equation, along with the knowledge of liquid volume and density, one can determine the surface tension and subsequently deduce the surfactant concentration in the solution (using calibration curves). It is important to note that this method is applicable only when a single known surfactant is present in the solution, as is the case for our experiments. Further details on quantifying the surfactant concentrations in water using surface tension and the use of pendent drop tensiometry can be found in previous publications[37,38]. Surface tension values were then converted to concentration using an experimentally obtained calibration curve for each respective PFCA standard (Fig. S3). If the

PFCA concentration in the solution exceeded its critical micellar concentration (CMC) or fell outside the linear range of the calibration curve, the solution was diluted by a known factor, which was later applied to estimate PFCA concentration in the bulk solution[36]. Additionally, the contact angle of water on PE was obtained using the sessile droplet mode of the same optical tensiometer/goniometer. The measurements were performed using a 5 μL sessile droplet of DI water placed on 1 cm^2 PE pellet. Images were captured and subsequently analyzed, from which the values of the contact angle were obtained.

2.3 ATR-FTIR spectroscopy

Attenuated total reflection Fourier-transform infrared spectroscopy (ATR-FTIR) was performed on (1) Pristine PE, (2) Pure C10 PFCA and (3) PE with adsorbed C10 PFCA. Results were obtained using a monolithic diamond crystal ATR accessory on a Bruker Alpha FTIR instrument. The instrument was blanked against the air, and subsequent measurements were taken by collecting 32 scans per spectrum at a 4 cm^{-1} resolution.

2.4 Accelerated weathering experiments

Natural sunlight was simulated by employing an Xe-1 weathering chamber (Q-Labs) equipped with a 340 nm wavelength filter and a corresponding irradiance set at 0.35 W m^{-2}, tested and calibrated according to the ASTM D5071 standard[39]. For the model PE MPs, a typical experiment was carried out by adding 10 mg of MPs into respective PFCA solutions. The concentration of the PFCA solutions coincided with ~70% of the maximum surface excess of each PFCA, which was calculated from the adsorption isotherms (see section 3.1). For the commodity macroplastics, each sample was placed in an excess solution of C8 PFCA and the surface excess was then estimated via calibration curve. The samples were then dried for 24 hours. After drying, each sample was placed in 1 mL of clean DI water within a sealed quartz cuvette, then subsequently placed in the weathering chamber for 10 days. The amount of C8 PFCA that was released back into the aqueous media was then estimated, using the same experimental calibration curves. Control experiments were also carried out in the absence of UV light, and in complete darkness.

2.5 Electrophoretic mobility

Electrophoresis of the PE MPs was performed using coplanar gold electrodes synthesized by deposition of gold vapor on a microscope glass slide. The slide was soaked in NoChromix (Godax) solution for 12 h and subsequently washed with DI water. A 5 mm wide paper mask was placed on the glass slide prior to coating the slide with a 10 nm layer of chromium followed by a 100 nm layer of gold in a vacuum metal evaporator (Thermionics VE-90). The aqueous suspension of MPs was then placed in the gap created by the paper mask between the gold electrodes. The direct current (DC) electric field was applied and manipulated by connecting the electrodes to a power supply (BK Precision 1665). The movement of the microplastics under the influence of electric field was monitored using Leica DM6000 optical microscope in brightfield mode.

3. Results and Discussion

3.1 Adsorption of PFCAs on microplastics

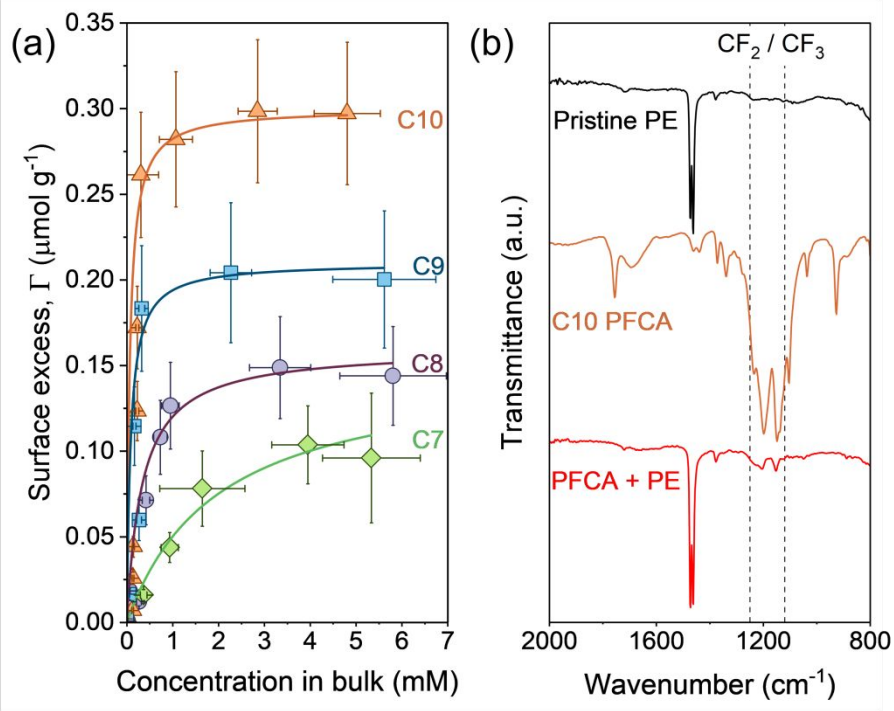

Figure 2. Adsorption of PFCAs onto MPs. (a) Isotherms for the adsorption of C7-C10 PFCAs onto MPs at 25ºC as a function of their equilibrium concentration in the bulk of solution. The symbols represent experimental surface excess normalized with the weight of MPs, and the lines are the corresponding best fits using the Langmuir adsorption isotherm model. The error bars in the abscissa and ordinate represent standard deviation of at least three experimental measurements. (b) The ATR-FTIR spectra of pristine PE, pure C10, and MPs with adsorbed C10. The vertical dashed lines at 1150 cm^{-1} and 1240 cm^{-1} span the area representing the fluoroalkyl region of the ATR-FTIR spectra.

To identify the impact of the fluoroalkyl chain length of PFCAs on their ability to bind to plastic surfaces, we experimentally measured the isotherms for adsorption of C7-C10 PFCAs on the MPs using surface tension measurements and the well-established solvent depletion method[34,40]. In a typical adsorption isotherm experiment, 10 mg of MPs were added to DI water containing known concentration of the PFCA (0.01-10 mM). After reaching equilibrium, the MPs with the adsorbed PFCA are then separated from the aqueous solvent using a syringe filter of pore size 0.45 μm. The amount of the unadsorbed PFCA in the filtrate is determined by measuring its surface tension using an optical tensiometer as detailed in section 2.2. The amount of PFCA adsorbed on the surface of MPs (Γ) is represented in μmol adsorbed per gram of MPs, and is estimated as $\Gamma = (c_0 - c)/m_{\mathrm{MPs}}$, where c_0 is the initial concentration of the PFCA in the water, c is the equilibrium concentration of PFCA in the filtrate (bulk) and m_{MPs} is the mass of the added MPs. The experimentally measured isotherms for adsorption of PFCAs with C7-C10 tail length onto PE MPs are shown in Figure 2a. We find that the amount of PFCA adsorbed increases rapidly with increasing equilibrium concentration, and then saturates to a constant value which corresponds to the maximum surface excess (Γ_{max}) (Fig. 2a). In the experiments, we find that the C10 PFCA has the

highest Γ_{max} for the MPs, adsorbing ~33% more than C9 and ~50% more than C8, while C7 showed the lowest adsorption on the MPs. While the environmental levels of PFCAs are typically lower than the concentrations used in our study, legacy AFFF can contain concentrations ranging from 0.3 to 19 mM for fluorinated C8 surfactants (such as PFOA and PFOS) and 0.1 and 0.4 mM for fluorinated C7 surfactants (such as PFHpA and PFHpS)[41–43]. Field studies near AFFF impacted areas have reported concentrations of the fluorinated surfactants in groundwater, surface water, and soil that fall within this range[42–44]. Since AFFFs often act as point sources for PFCA contamination, our experimental concentrations retain environmental significance and have important implications for understanding the fate and effects of PFCA in the environment. However, the primary purpose of our study is to shed light on the fundamental interactions between the PFCAs and the plastic substrates, and their corresponding impacts on the properties of MPs.

The experimental adsorption isotherms were further analyzed using the Langmuir adsorption model. This two-parameter model is applicable under the assumption of monolayer adsorption of PFCAs on MPs, and the existence of a dynamic equilibrium between the adsorbed and unabsorbed state of the PFCA. Under such assumptions the surface excess is given as:

$$\Gamma = \frac{\Gamma_{max} K_{ads} c_o}{1 + K_{ads} c_o} \quad (1)$$

where K_{ads} is the equilibrium adsorption constant, which is proportional to the binding affinity of PFCAs to the MPs. The experimental data is fitted using equation 1, with Γ_{max} and K_{ads} as fit parameters. The values obtained for maximum surface excess and adsorption constant as a function of number of carbon atoms in the tail of PFCAs are shown in Table 1.

Table 1. Adsorption isotherm fitting parameter obtained using Langmuir model.

PFCAs	Γ_{max} (µmol g^{-1})	K_{ads} (×1000 M^{-1})
C7	0.10	0.5
C8	0.15	2.0
C9	0.20	12.0
C10	0.30	16.8

We report an increase in the values of Γ_{max}, and K_{ads} with increasing number of C-atoms in the fluoroalkyl chain of the model PFCAs (Table 1). This observed increase in Γ_{max} can be attributed to the increase in the hydrophobic attraction between the longer chain PFCAs and the MPs surface leading to a closer packing of the molecules at the interface. The increase in binding affinity of PFCAs onto neutral MPs can be quantified by the Gibbs free energy of adsorption (ΔG^o_{ads}) from K_{ads} as $\Delta G^o_{ads} = -N_A k_B T \ln(K_{ads})$ where N_A is the Avogadro number, k_B is the Boltzmann constant, and T is the temperature[45]. We observe an increase in ΔG^o_{ads} from -15 kJ mol^{-1} to -24 kJ mol^{-1} upon increasing the number of C-atoms in the tail of the PFCA, which are consistent with existing literature on the binding of molecules onto solid-liquid interfaces[45]. We report an increasing affinity of PFCAs for microplastic surface with increasing fluoroalkyl chain length. This observation aligns with current literature which reports a correlation with chain length and adsorption onto environmental media such as minerals[46,47], and soils[48,49] as well as its

bioaccumulation in plants[50]. Our results further demonstrate how the chemical structure of PFCAs influences their adsorption to environmental media, particularly through hydrophobic interactions between the adsorbent and adsorbate. Note that the model PFCAs used in the study are acidic in nature and affect the pH of solutions.

Increasing the concentration of PFCAs will lead to a decrease in the pH of the solution. This is due to the release of protons upon the dissociation of carboxylic acid headgroup of the PFCAs, causing an acidic shift. At acidic pH, the nonionic and anionic forms of the PFCA molecule will exist in equilibrium (below the equivalence point). As the pH increases beyond the equivalence point, the ionized carboxylate state i.e. anionic form of the PFCAs solely will be present in the solution. This behavior has been established for fatty acid molecules[51], and PFCAs are anticipated to behave in a similar manner. Hence, the pH could impact the adsorption of PFCAs, especially onto charged surfaces. The current study uses DI water as the solvent, where the pH varies with the concentration of PFCAs. Here the use of buffer solutions was intentionally avoided as increasing the ionic strength (due to the presence of buffers) will not only alter the interactions of the PFCA with MPs but also influence the hydrophobic interactions between the tails of the PFCA molecules and impact corresponding adsorption behavior[36]. Further work is needed to delineate the roles of pH, ionic strength, and ionization state of the headgroup on the adsorption of PFCAs onto solid-liquid interfaces.

The mechanism of adsorption of PFCAs on MPs primarily relies on the hydrophobic interactions between the tail of the PFCAs and the hydrophobic MP surface. Since the adsorption is mainly driven by these nonpolar interactions, the influence of pH, which primarily affects the ionization state of the headgroup, is expected to be minimal in this scenario. The pristine polyethylene in its near neutral charged state is not anticipated to electrostatically interact with PFCA molecules. We further ascertain this conjecture by measuring the adsorption isotherm for C8 PFCA onto MPs at pH 7 and 0.6 M NaCl i.e. salinity equivalent to ocean water (Fig. S4). The isotherms measured at pH 7 and elevated salinity remains nearly the same to the isotherm in DI water, presumably due to the strong hydrophobic attraction between the plastic surface and the fluorinated tail of the PFCA. Notably, the interfacial activity of PFOA is reduced as the solution pH is increased (Fig. S4a), likely due to the alteration in the ionization state of the headgroup; however, further research is required to validate this hypothesis conclusively. This invariance of PFCA adsorption on plastics further highlights that the conclusions of our controlled lab-based study will be valid under real environmental conditions.

Adsorption of PFCAs lead to significant changes in the surface of the MPs. We employ ATR-FTIR to probe the presence of PFCA on the surface using vibrational spectroscopy on a 1 cm × 1 cm pellet formed by thermal molding the PE MPs[52]. The PE pellet was submerged in a solution containing excess of C10 PFCA (5 mM) and allowed to equilibrate for 24 hours. After equilibration, the pellet was removed from the PFCA solution, and dried for 12 hours at room temperature before acquiring the ATR-FTIR spectra. Air-drying at room temperature is a suitable method for this particular system because of the chemically inert nature of polyethylene, which makes prolonged exposure to air unlikely to cause any degradation or changes to the chemical signature. C10 was selected as the model PFCA due to its high affinity for adsorption onto MPs,

which makes ensuing changes in the ATR-FTIR spectra easier to detect relative to shorter-chained PFCAs. The ATR-FTIR spectra of the pristine plastic pellet, pure C10 PFCA, and PE pellet with adsorbed C10 PFCA are shown in Figure 2b (see Fig. S5 for complete spectra). We find that adsorption of C10 onto PE pellet introduces distinct peaks in the region 1150-1240 cm^{-1} in the ATR-FTIR spectra, corresponding to the C-F streching[53,54]. The emergence of these peaks in the spectra of PE pellet confirms the adsorption of the PFCA on the surface of the plastic.

3.2 Effect of PFCA adsorption on the dispersity of MPs

PFCAs adsorb onto MPs with their hydrophilic head group facing the aqueous solvent. This corollary is based on the observed increase in the maximum surface excess of adsorbed PFCA upon increasing the carbon atom tail length (Fig. 2a), combined with the existing literature for surfactant adsorption on hydrophobic surfaces[55]. The adsorption of PFCAs can influence the wettability of the MPs and lead to alterations in their transport behavior in the aqueous media (Fig. 3). In the absence of PFCAs, we find that the neutrally buoyant MPs are situated at the air-water interface. This flotation of the MPs is due to their hydrophobicity rather than their mass density being lower than water. However, upon the addition of PFCA (here C8), we observe a significant increase in the dispersibility of MPs in the water column (Fig. 3a). In this instance, C8 was chosen as the model PFCAs for the experiment due to its significant environmental relevance, but it should be noted that this behavior was observed for all C7 to C10 PFCAs (Fig. S6). We quantify the change in dispersity of the MPs upon the addition of the PFCA by estimating the number density of the MPs in the water column using ImageJ software package[56]. In a typical image analysis, the number of MPs particles per mm^2 of the image are determined and plotted as a function of the amount of PFCA. We find a rapid increase in the number density of the MPs dispersed in water with increasing the C8 PFCA concentration (Fig. 3b). The change in water wettability of the MPs due to the adsorption of PFCAs drives the observed changes in the dispersibility of MPs in aqueous media.

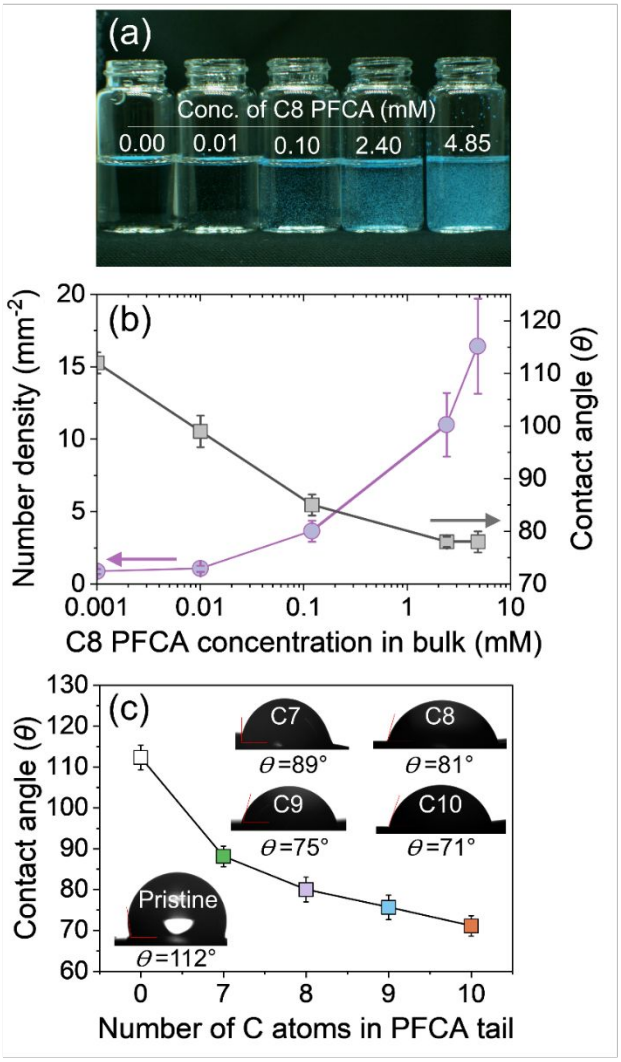

Figure 3. Effect of PFCA adsorption on the wettability and dispersity of MPs. (a) Image showing the increased dispersibility of MPs upon increasing the concentration of C8 PFCA. (b) Increase in number density of microplastics in the bulk of solution (circles) and decrease in the water contact angle of PE pellet (squares) upon increase in the concentration of C8 PFCA. The pellet was formed by thermal molding of the PE MPs. (c) Decrease in the water contact angle as function of the number of carbon atoms in the fluoroalkyl chain of each PFCA. The pellets were equilibrated in respective 5 mM solution of the PFCAs. Insets show the water droplet on the surface of the pellet. The error bars in (b) and (c) represent the standard deviation of at least three experiments.

The wettability of the MPs is experimentally quantified by measuring the contact angle (θ) of a water droplet on the centimeter sized PE pellets formed by thermal molding of the PE MPs. The PE pellets are submerged in solutions containing increasing amounts of C8 PFCA and allowed to equilibrate for 24 hours. After drying, we measured the contact angle of a 5 µL droplet of water on the pellet using an optical goniometer. We find that the water contact angle decreases with increasing the concentration of C8 PFCA (Fig. 3b), highlighting the transition of the PE surface from hydrophobic to hydrophilic. The increase in the water wettability of the MPs upon the adsorption of PFCAs is the reason for observed increase in their dispersity in water (Fig. 3a-b).

Additionally, we find that the water wettability of the PE pellet saturated with PFCA is dependent on the number of carbon atoms in the fluoroalkyl tail. The contact angle shows a decrease with increasing the number of carbon atoms in the tail from C7 to C10 (Fig. 3c). The decrease in contact angle with increasing PFCA tail length is due to the increase in the Γ_{max} of the PFCA adsorbed on the PE surface (Fig. 2a). Our wettability experiments indicate that the coexistence of MPs and PFCAs in an aqueous environment could lead to an increase in the vertical transport of MPs.

3.3 Desorption of PFCAs from MP surface upon weathering

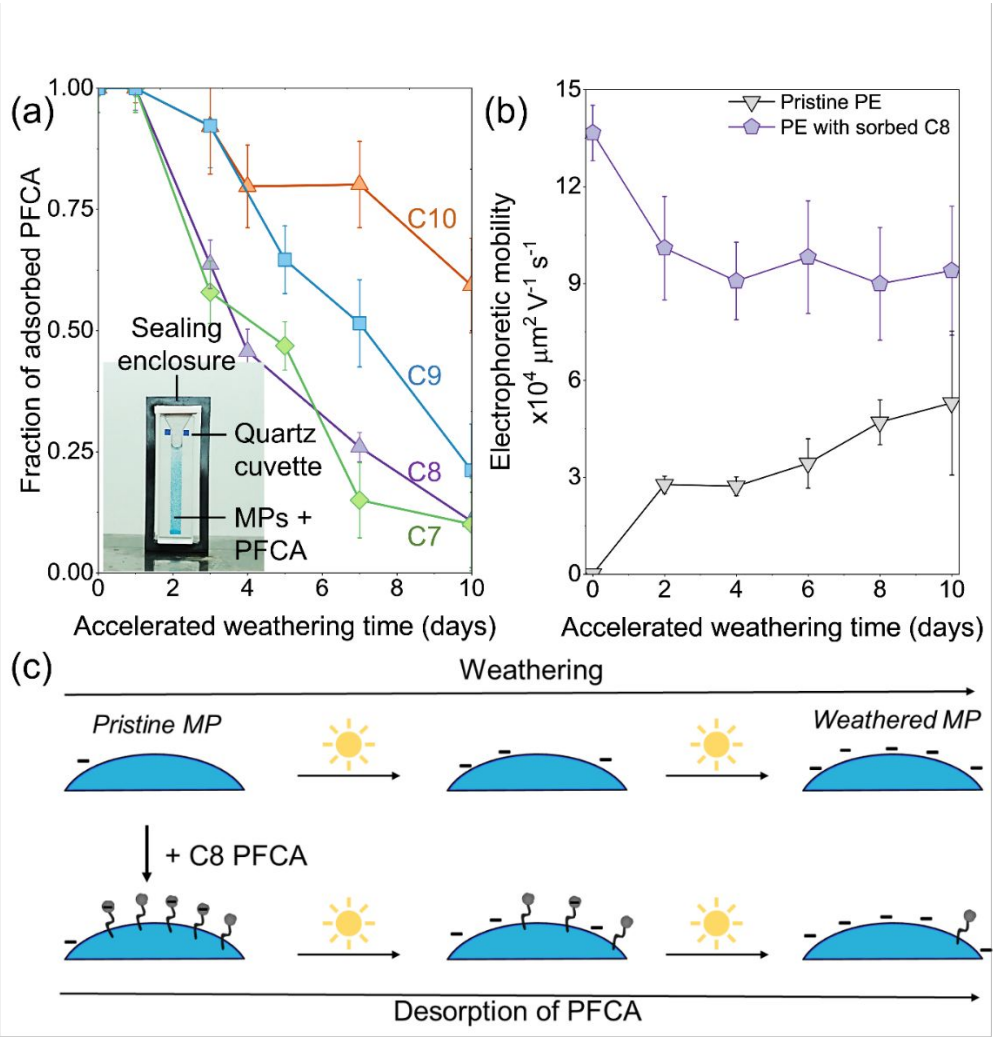

Figure 4: The sunlight-induced release of PFCAs from MPs. (a) The fraction of PFCAs remained adsorbed onto MPs upon increasing the time of accelerated weathering. The points represent experimental data, while the error bars are the standard deviation of at least three measurements. The inset is an image of the sealed quartz cuvette used for the weathering experiments. The cuvette contained the MPs with adsorbed PFCAs. (b) Changes in the electrophoretic mobility of MPs in their pristine form (triangles) i.e. no adsorbed PFCA and with adsorbed C8 PFCA (pentagons) as a function of the time spent in the accelerated weathering chamber. (c) Schematic representation of the mechanism for the weathering of microplastics (top) and the sunlight-induced desorption of C8 PFCA from the surface of the MPs (bottom).

Environmental stressors could alter the surface chemistry of the MPs, thus impacting the state of the pre-adsorbed PFCA molecules. Here, we investigate the effects of sunlight-induced photooxidation of MPs on the sorption behavior of PFCAs. We subject the MPs with pre-adsorbed PFCAs to photooxidation via an accelerated weathering chamber. Previously, we have shown that the photooxidation increases the density of negatively charged moieties on the surface of PE MPs[52]. The increase in negative charge density of PE MPs is due to the dissociation of carboxylic acid groups, which are the predominant photooxidative product formed on the plastic surface[57]. To understand the role of these newly formed photooxidized entities on the PFCA-MPs interactions, we investigated the change in the amount of PFCAs bound to the surface of MPs upon increasing incubation times in the accelerated weathering chamber. In a typical experiment, sealed quartz cuvettes were filled with 1 mL of a known C8 PFCA concentration corresponding to ~70% Γ_{max} for 10 mg of MPs (Fig. 2a, and Fig. 4a (inset)). The PFCA-MPs mixture was equilibrated for 24 hours on an orbital shaker (30 rpm), which allowed for the adsorption process to complete. The sealed quartz cuvettes containing the PFCA-MPs mixtures were then transferred to the weathering chamber.

In the accelerated weathering chamber, sunlight-driven photooxidation of plastics is simulated using a xenon arc lamp equipped with a filter that restricts UVB and UVC radiation, while favoring wavelengths in the UVA spectrum (~340 nm). The irradiance and temperature remain constant at 0.35 W m^{-2} and 63 °C, respectively, which generates an experimental environment that is comparable to natural sunlight, following the ASTM D5071 standard (see section 2.4)[39]. The combination of these parameters effectively accelerates the rate of photooxidation by a factor that can range from approximately 10 to 30 (as estimated by TenCate Geosynthetics[58]). However, the exact acceleration factor in the real world would depend on both spatial and topological parameters such as latitude and altitude. This means that 24 h of UV exposure inside the weathering chamber may correspond to between 10 and 30 days of exposure in a natural environment. To preserve simplicity and avoid inaccuracy, experimental results are reported as a function of accelerated weathering time. In our experiments, we monitor the change in adsorbed state of each PFCA bound to MPs for up to 10 days of accelerated weathering. This time interval is chosen because during this period significant changes in the surface chemistry of the MPs can be observed[52]. Additionally, there is no significant difference in the surface excess values for each PFCA after 10 days of equilibration without exposure to UV irradiation and in darkness (Fig. S7). MPs exposed beyond 10 days of accelerated weathering display signs of mechanical stress (i.e. cracking, fracturing)[52], which are not further investigated in this study.

The discrete negative charges introduced on the surface of the MPs due to sunlight-induced photooxidation drives the desorption of PFCAs from the surface of the plastics. The desorption isotherms of the four model PFCAs onto PE MPs are reported as a fraction of the initial surface excess, and accelerated weathering time (Fig. 4a). We find that the amount of surfactant bound to MPs decreases with increasing weathering time, i.e., PFCAs desorb from MPs throughout weathering. Additionally, we find that the release of PFCA molecules from the microplastic surface under simulated sunlight conditions is strongly dependent on the fluoroalkyl tail length. After 10 days of accelerated weathering, we report a ~40% decrease in the adsorbed amount of C10 PFCA, and ~90% decrease in both C7 and C8 PFCA (Fig. 4a). This correlates with the fact

that molecules with weaker hydrophobic attraction to the surface, such as shorter chained PFCAs, will desorb more easily[59]. Furthermore, the electrostatic repulsion between the negatively charged photooxidative products on the MP surface and the anionic head groups of the fluorinated surfactant would also contribute to the desorption process (Fig. 4c). We further anticipate that pH could potentially play a role in the desorption process. Note that complete desorption of PFCA from the MP surface was not observed within the tested 10 days. This finding is consistent with existing literature, which describes the complete desorption of surfactants from solid-liquid interfaces being exceptionally difficult[60]. In this instance, the photo-induced changes to the microplastic surface are site-specific, and therefore perhaps allowing the PFCA to remain adsorbed to less-affected sites on the MPs (Fig. 4c).

The surface charge density of MPs is altered by both the weathering process and adsorbed chemicals. To corroborate this, we investigate changes in the electrophoretic mobility of both pristine MPs and the MPs with adsorbed C8 PFCA as a function of accelerated weathering time. The electrophoretic mobility μ_E is the velocity v of a particle in an external electric field normalized to the applied field strength E, i.e. $\mu_E = v/E$. In this case, $v = (\varepsilon\zeta/\eta)E$, where ε is the dielectric constant of the medium, ζ is the zeta potential of the MP, and η is the viscosity of the medium. Therefore, μ_E is linearly proportional to the zeta potential and dependent on the surface charge density of the MP particles[61]. We performed the electrophoretic mobility measurements by transferring 100 µL of PFCA-MPs mixture in the 5 mm gap between two coplanar gold electrodes and applying 5 V of DC potential (see section 2.5).

Pristine unweathered MPs with no adsorbed PFCAs show no significant migration towards either electrode indicating the lack of charge on the surface of MPs. Upon weathering, the pristine MPs in the DC field migrate towards anode highlighting the negative surface potential of the MP surface. The electrophoretic mobility increases with increasing weathering time, indicating the increase in the negative surface charge density on MPs (Fig. 4b). The observed increase in μ_E of MPs upon weathering in the absence of PFCA is attributed to the formation of carboxylate ions and other negatively charged functional groups on the surface of PE due to photooxidation, as discussed in our previous publication[52].

Addition of C8 PFCA to pristine unweathered MPs increases the μ_E significantly. The MPs migrate toward the anode, indicating that the net surface charge of MPs with adsorbed C8 PFCA is negative. Interestingly, the value of μ_E decreases with increasing weathering time and remains larger than MPs weathered in the absence of the C8 PFCA (Fig. 4b). The net electrophoretic mobility of the MPs is governed by two factors: (I) Oxidation state of the MPs surface, and (II) Amount of the PFCA adsorbed on the MPs. Weathering driven photooxidation leads to the charging of the PE surface, which drives the desorption of the C8 PFCA molecules (Fig. 4a-b). The PFCA desorption upon weathering could lead to the observed decrease in the μ_E of the MPs. In summary, the weathering of MPs drives the formation of negative charges on their surface, which in-turn triggers the release of pre-adsorbed PFCA molecules from MPs surface (Fig. 4c). The adsorption/desorption of PFCAs from the surface of MPs could have a significant impact on their mutual transport in the environment. Additionally, the change in surface properties of MPs will influence their life cycle in the environment and affect both their behavior and interactions

with the surrounding environment. Existing literature has reported that the presence of surfactant can influence the ability of MPs to adsorb other chemicals such as antibiotics[62], ionic contaminants[63] and hydrophilic pollutants[64].

3.4 Uptake and release of PFCAs from commodity plastics

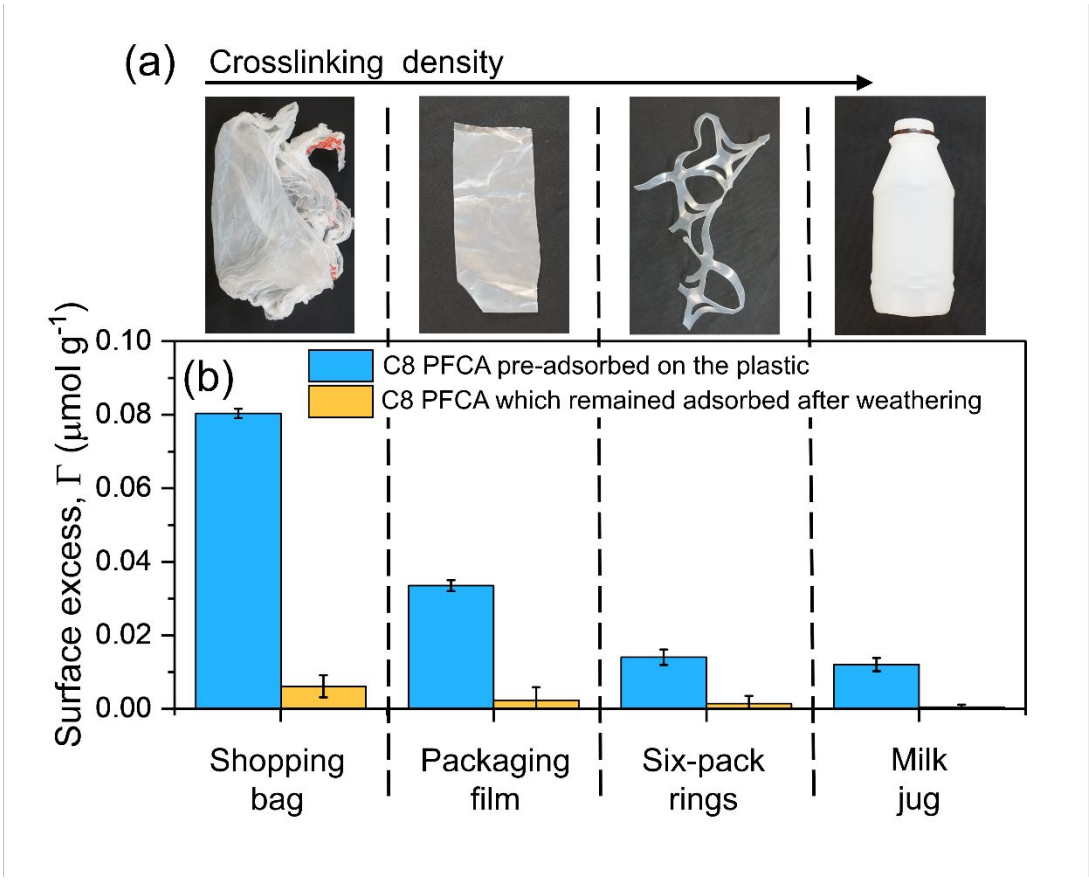

Figure 5. Uptake and release of C8 PFCA from commodity plastics. (a) Images of the commodity macroplastics used in the experiments in the order of their crosslinking density. (b) The amount of C8 PFCA adsorbed onto the plastics (blue) and the amount that remained adsorbed after 10 days of accelerated weathering (yellow). Error bars represent the standard deviation of three measurements.

Our findings indicate an intricate relationship between PFCAs and MPs, where the weathering state of the plastic could impact the PFCA adsorption/desorption behavior. We further investigate the relation between PFCAs sorption characteristics and weathering state of plastics by testing the uptake and release of C8 PFCA from four commodity PE macroplastics. These plastics included: (1) a shopping bag, (2) a thin film for packaging, (3) six-pack rings for holding beverages and (4) a milk jug. The wettability characteristics and thickness of each plastic are provided in Figure S8 and S9. These model commodity plastics were selected due to their widespread use in consumer products, as well as their accessibility. Note that all these commodity plastics are chemically PE,

but the crosslinking density of the polymer chains forming these model materials vary significantly. Here the purpose of investigating these commodity materials is to elucidate the broader impact of plastic weathering on PFCA sorption behavior. In a typical experiment, a known amount of the commodity plastic is added to a concentrated solution of C8 PFCA and allowed to equilibrate for 24 hours. During this period, surface of the plastic is saturated with the PFCA molecules, i.e., respective Γ_{max} is attained. The commodity plastic with adsorbed C8 PFCA molecules is then dried overnight at room temperature and weathered for 10 days as described in section 3.3.

We find that the shopping bag adsorbed the maximum amount of the C8 PFCA, followed by the packaging film, six-pack rings, and the milk jug. (Fig. 5b). The systematic decrease in the adsorbed amount could be attributed to the change in the specific surface area of the plastics in the order shopping bag > packaging film > six-pack rings > milk jug, which is based on the observed thickness of the material (Fig. S9). After 10 days of accelerated weathering, the pre-adsorbed C8 PFCA is subsequently released back into the aqueous solution (Fig. 5b). The amount of the C8 PFCA which remains bound to the surface after weathering decreases in all tested commodity plastics. The shopping bag retained the most PFCA followed by the packaging film, then the six-pack rings, while the milk jug retained the least. The desorption is again attributed to the change in surface chemistry of the MPs due to photooxidation (Fig. 4c). Note that the chemical composition and nature of additives used in the manufacturing of the commodity plastics used in our study may not be identical. Despite such inherent variability, all commodity plastics show an initial adsorption and subsequent weathering-induced release of PFCA molecules. Therefore, one generic conclusion which can be drawn is that regardless of the exact composition, thickness and size, PE plastics tend to uptake PFCAs, and release upon weathering. Further work is necessary to identify the exact composition of the commodity plastics and its relationship with the sorption behavior of PFCAs.

4. Conclusions and perspective

In the present study, we have demonstrated (1) the ability of PFCAs to adsorb onto polyethylene (PE) micro and macroplastics (MPs); (2) the effect of PFCAs on the wettability and dispersibility of MPs; and (3) the desorption of PFCAs from the plastics upon sunlight-induced weathering. The adsorption of the PFCAs is governed by hydrophobic interactions between the PFCA fluoroalkyl tail and plastic surface. Adsorbed PFCAs impact both the wettability and dispersibility of the model PE MPs. This specific aspect points to the potential role of PFCAs in the vertical migration and transport of MPs in aquatic environments, where the two contaminants can coexist. Finally, we identify the role of sunlight in the desorption of PFCAs from the MP surface. The desorption of PFCA from micro and macroplastics is driven by the increase in hydrophilicity of MPs and repulsion between the PFCA and photooxidized plastic surface. Analogous to the adsorption mechanism, the desorption of PFCAs is highly dependent on fluoroalkyl chain length; longer chained PFCA molecules can overcome the electrostatic repulsion, while shorter chained PFCAs are more susceptible to be released from the MP surface. The uptake and release of PFCAs from plastics highlights the role of MPs as a vector of transport for PFCAs in the environment, and a potential route of exposure for marine biota. The lab-based experiments described in the present

article focus on the fundamental mechanisms that drive the interactions between the two emerging contaminants. The trends observed in our study are in good agreement with statistical models that have been employed to describe the potential relationship between PFCAs and MPs[22], while also accounting for sunlight-induced alterations to their interactions. It should be noted that simulated sunlight in the laboratory does not always reflect true environmental processes, due to non-reproducible factors such as fluctuations in humidity, UV index and wind conditions. However, the true value in these experiments lies within the fundamental knowledge gained by observing the sunlight-induced alterations to the surface of plastics and corresponding change in PFCA sorption process. Further research is required to provide more context on the life cycle of coexisting microplastics and PFCAs in different environmental conditions. Additionally, the presence of electrolytes, counterions, biofilms on the plastic surface, additives in plastics and mixed salts in natural seawater will impact the adsorptive behavior of surfactants and will likely alter the interactions between MPs and PFCAs[35,65]. Finally, it may be warranted to investigate the adsorption of PFCAs onto a particle surface at various point sources (i.e., AFFF impacted areas), that could contain perfluorinated surfactants at concentrations equal to or exceeding the critical micelle concentration (CMC). This is because at higher concentrations, surfactants have the ability to form distinct structures at solid-liquid interfaces, which influence the substrates[66]. Although a quantitative assessment on the simultaneous presence of MPs and PFCAs at point sources currently lacking, circumstantial evidence suggests their likely coexistence. For instance, military bases, a known common point source of AFFF deposition in the environment[42,43], also pose specific concerns regarding solid waste management[67]. Considering the urbanized atmosphere of military facilities and their historical use of AFFFs on-site, it is plausible that both microplastic pollutants and PFCAs could be concentrated in the same areas. The potential coexistence of microplastic pollutants and PFCAs at AFFF impacted sites warrants further investigation in the field, to fully comprehend their interplay. Our study provides fundamental knowledge on the complex relationship between the two emerging contaminants and the dependence of this relationship on environmental stress, here sunlight-induced weathering.

Competing Interests: The authors do not declare any competing interests.

Acknowledgements: Authors acknowledge the Division of Chemistry at the National Science Foundation (MPS-2032497) for financial support.

5. References

(1) Andrady, A. L. Microplastics in the Marine Environment. *Mar Pollut Bull* **2011**, *62* (8), 1596–1605. https://doi.org/https://doi.org/10.1016/j.marpolbul.2011.05.030.

(2) Petersen, F.; Hubbart, J. A. The Occurrence and Transport of Microplastics: The State of the Science. *Science of The Total Environment* **2021**, *758*, 143936. https://doi.org/https://doi.org/10.1016/j.scitotenv.2020.143936.

(3) Sharma, S.; Sharma, B.; Dey Sadhu, S. Microplastic Profusion in Food and Drinking Water: Are Microplastics Becoming a Macroproblem? *Environ Sci Process Impacts* **2022**, *24* (7), 992–1009. https://doi.org/10.1039/D1EM00553G.

(4) Al Harraq, A.; Bharti, B. Microplastics through the Lens of Colloid Science. *ACS Environmental Au* **2022**, *2* (1), 3–10. https://doi.org/10.1021/acsenvironau.1c00016.

(5) Velzeboer, I.; Kwadijk, C. J. A. F.; Koelmans, A. A. Strong Sorption of PCBs to Nanoplastics, Microplastics, Carbon Nanotubes, and Fullerenes. *Environ Sci Technol* **2014**, *48* (9), 4869–4876. https://doi.org/10.1021/es405721v.

(6) Joo, S. H.; Liang, Y.; Kim, M.; Byun, J.; Choi, H. Microplastics with Adsorbed Contaminants: Mechanisms and Treatment. *Environmental Challenges* **2021**, *3*, 100042. https://doi.org/https://doi.org/10.1016/j.envc.2021.100042.

(7) Vockenberg, T.; Wichard, T.; Ueberschaar, N.; Franke, M.; Stelter, M.; Braeutigam, P. The Sorption Behaviour of Amine Micropollutants on Polyethylene Microplastics – Impact of Aging and Interactions with Green Seaweed. *Environ Sci Process Impacts* **2020**, *22* (8), 1678–1687. https://doi.org/10.1039/D0EM00119H.

(8) Santillo, D.; Miller, K.; Johnston, P. Microplastics as Contaminants in Commercially Important Seafood Species. *Integr Environ Assess Manag* **2017**, *13* (3), 516–521. https://doi.org/https://doi.org/10.1002/ieam.1909.

(9) EPA. *PFAS Explained*. https://www.epa.gov/pfas/pfas-explained.

(10) Glüge, J.; Scheringer, M.; Cousins, I. T.; DeWitt, J. C.; Goldenman, G.; Herzke, D.; Lohmann, R.; Ng, C. A.; Trier, X.; Wang, Z. An Overview of the Uses of Per- and Polyfluoroalkyl Substances (PFAS). *Environ Sci Process Impacts* **2020**, *22* (12), 2345–2373. https://doi.org/10.1039/D0EM00291G.

(11) Valsecchi, S.; Rusconi, M.; Mazzoni, M.; Viviano, G.; Pagnotta, R.; Zaghi, C.; Serrini, G.; Polesello, S. Occurrence and Sources of Perfluoroalkyl Acids in Italian River Basins. *Chemosphere* **2015**, *129*, 126–134. https://doi.org/https://doi.org/10.1016/j.chemosphere.2014.07.044.

(12) Yeung, L. W. Y.; Dassuncao, C.; Mabury, S.; Sunderland, E. M.; Zhang, X.; Lohmann, R. Vertical Profiles, Sources, and Transport of PFASs in the Arctic Ocean. *Environ Sci Technol* **2017**, *51* (12), 6735–6744. https://doi.org/10.1021/acs.est.7b00788.

(13) Kim, Y.; Pike, K. A.; Gray, R.; Sprankle, J. W.; Faust, J. A.; Edmiston, P. L. Non-Targeted Identification and Semi-Quantitation of Emerging per- and Polyfluoroalkyl Substances (PFAS) in US Rainwater. *Environ Sci Process Impacts* **2023**. https://doi.org/10.1039/D2EM00349J.

(14) EPA. *Drinking Water Health Advisories for PFOA and PFOS*. https://www.epa.gov/sdwa/drinking-water-health-advisories-pfoa-and-pfos.

(15) Steenland, K.; Winquist, A. PFAS and Cancer, a Scoping Review of the Epidemiologic Evidence. *Environ Res* **2021**, *194*, 110690. https://doi.org/https://doi.org/10.1016/j.envres.2020.110690.

(16) Cao, Y.; Ng, C. Absorption, Distribution, and Toxicity of per- and Polyfluoroalkyl Substances (PFAS) in the Brain: A Review. *Environ Sci Process Impacts* **2021**, *23* (11), 1623–1640. https://doi.org/10.1039/D1EM00228G.

(17) Jian, J.-M.; Chen, D.; Han, F.-J.; Guo, Y.; Zeng, L.; Lu, X.; Wang, F. A Short Review on Human Exposure to and Tissue Distribution of Per- and Polyfluoroalkyl Substances (PFASs). *Sci Total Environ* **2018**, *636*, 1058–1069. https://doi.org/10.1016/j.scitotenv.2018.04.380.

(18) Scott, J. W.; Gunderson, K. G.; Green, L. A.; Rediske, R. R.; Steinman, A. D. Perfluoroalkylated Substances (PFAS) Associated with Microplastics in a Lake Environment. *Toxics* **2021**, *9* (5), 106. https://doi.org/10.3390/toxics9050106.

(19) Kumar, R.; Vuppaladadiyam, A. K.; Antunes, E.; Whelan, A.; Fearon, R.; Sheehan, M.; Reeves, L. Emerging Contaminants in Biosolids: Presence, Fate and Analytical Techniques. *Emerg Contam* **2022**, *8*, 162–194. https://doi.org/https://doi.org/10.1016/j.emcon.2022.03.004.

(20) Borthakur, A.; Leonard, J.; Koutnik, V. S.; Ravi, S.; Mohanty, S. K. Inhalation Risks of Wind-Blown Dust from Biosolid-Applied Agricultural Lands: Are They Enriched with Microplastics and PFAS? *Curr Opin Environ Sci Health* **2022**, *25*, 100309. https://doi.org/https://doi.org/10.1016/j.coesh.2021.100309.

(21) Manzetti, S.; van der Spoel, D. Impact of Sludge Deposition on Biodiversity. *Ecotoxicology* **2015**, *24* (9), 1799–1814. https://doi.org/10.1007/s10646-015-1530-9.

(22) Hatinoglu, M. D.; Perreault, F.; Apul, O. G. Modified Linear Solvation Energy Relationships for Adsorption of Perfluorocarboxylic Acids by Polystyrene Microplastics. *Science of The Total Environment* **2023**, *860*, 160524. https://doi.org/https://doi.org/10.1016/j.scitotenv.2022.160524.

(23) Kancharla, S.; Alexandridis, P.; Tsianou, M. Sequestration of Per- and Polyfluoroalkyl Substances (PFAS) by Adsorption: Surfactant and Surface Aspects. *Curr Opin Colloid Interface Sci* **2022**, *58*, 101571. https://doi.org/https://doi.org/10.1016/j.cocis.2022.101571.

(24) Ateia, M.; Zheng, T.; Calace, S.; Tharayil, N.; Pilla, S.; Karanfil, T. Sorption Behavior of Real Microplastics (MPs): Insights for Organic Micropollutants Adsorption on a Large Set of Well-Characterized MPs. *Science of The Total Environment* **2020**, *720*, 137634. https://doi.org/https://doi.org/10.1016/j.scitotenv.2020.137634.

(25) Erni-Cassola, G.; Zadjelovic, V.; Gibson, M. I.; Christie-Oleza, J. A. Distribution of Plastic Polymer Types in the Marine Environment; A Meta-Analysis. *J Hazard Mater* **2019**, *369*, 691–698. https://doi.org/10.1016/j.jhazmat.2019.02.067.

(26) Buck, R. C.; Franklin, J.; Berger, U.; Conder, J. M.; Cousins, I. T.; de Voogt, P.; Jensen, A. A.; Kannan, K.; Mabury, S. A.; van Leeuwen, S. P. J. Perfluoroalkyl and Polyfluoroalkyl Substances in the Environment: Terminology, Classification, and Origins. *Integr Environ Assess Manag* **2011**, *7* (4), 513–541. https://doi.org/https://doi.org/10.1002/ieam.258.

(27) Costanza, J.; Arshadi, M.; Abriola, L. M.; Pennell, K. D. Accumulation of PFOA and PFOS at the Air–Water Interface. *Environ Sci Technol Lett* **2019**, *6* (8), 487–491. https://doi.org/10.1021/acs.estlett.9b00355.

(28) van der Schyff, V.; Kwet Yive, N. S. C.; Polder, A.; Cole, N. C.; Bouwman, H. Perfluoroalkyl Substances (PFAS) in Tern Eggs from St. Brandon's Atoll, Indian Ocean. *Mar Pollut Bull* **2020**, *154*, 111061. https://doi.org/https://doi.org/10.1016/j.marpolbul.2020.111061.

(29) Houde, M.; Wells, R. S.; Fair, P. A.; Bossart, G. D.; Hohn, A. A.; Rowles, T. K.; Sweeney, J. C.; Solomon, K. R.; Muir, D. C. G. Polyfluoroalkyl Compounds in Free-Ranging Bottlenose Dolphins (Tursiops Truncatus) from the Gulf of Mexico and the Atlantic Ocean. *Environ Sci Technol* **2005**, *39* (17), 6591–6598. https://doi.org/10.1021/es0506556.

(30) Joerss, H.; Xie, Z.; Wagner, C. C.; von Appen, W.-J.; Sunderland, E. M.; Ebinghaus, R. Transport of Legacy Perfluoroalkyl Substances and the Replacement Compound HFPO-DA through the Atlantic Gateway to the Arctic Ocean—Is the Arctic a Sink or a Source? *Environ Sci Technol* **2020**, *54* (16), 9958–9967. https://doi.org/10.1021/acs.est.0c00228.

(31) Cui, J.; Gao, P.; Deng, Y. Destruction of Per- and Polyfluoroalkyl Substances (PFAS) with Advanced Reduction Processes (ARPs): A Critical Review. *Environ Sci Technol* **2020**, *54* (7), 3752–3766. https://doi.org/10.1021/acs.est.9b05565.

(32) Bressel, K.; Prevost, S.; Appavou, M.-S.; Tiersch, B.; Koetz, J.; Gradzielski, M. Phase Behaviour and Structure of Zwitanionic Mixtures of Perfluorocarboxylates and Tetradecyldimethylamine Oxide—Dependence on Chain Length of the Perfluoro Surfactant. *Soft Matter* **2011**, *7* (23), 11232–11242. https://doi.org/10.1039/C1SM05618B.

(33) Lee, J. G.; Larive, L. L.; Valsaraj, K. T.; Bharti, B. Binding of Lignin Nanoparticles at Oil–Water Interfaces: An Ecofriendly Alternative to Oil Spill Recovery. *ACS Appl Mater Interfaces* **2018**, *10* (49), 43282–43289. https://doi.org/10.1021/acsami.8b17748.

(34) Ma, Y.; Wu, Y.; Lee, J. G.; He, L.; Rother, G.; Fameau, A.-L.; Shelton, W. A.; Bharti, B. Adsorption of Fatty Acid Molecules on Amine-Functionalized Silica Nanoparticles: Surface Organization and Foam Stability. *Langmuir* **2020**, *36* (14), 3703–3712. https://doi.org/10.1021/acs.langmuir.0c00156.

(35) Pete, A. J.; Brahana, P. J.; Bello, M.; Benton, M. G.; Bharti, B. Biofilm Formation Influences the Wettability and Settling of Microplastics. *Environ Sci Technol Lett* **2022**. https://doi.org/10.1021/acs.estlett.2c00728.

(36) Ma, Y.; Heil, C.; Nagy, G.; Heller, W. T.; An, Y.; Jayaraman, A.; Bharti, B. Synergistic Role of Temperature and Salinity in Aggregation of Nonionic Surfactant-Coated Silica Nanoparticles. *Langmuir* **2023**, *39* (16), 5917–5928. https://doi.org/10.1021/acs.langmuir.3c00432.

(37) Beverung, C. J.; Radke, C. J.; Blanch, H. W. Protein Adsorption at the Oil/Water Interface: Characterization of Adsorption Kinetics by Dynamic Interfacial Tension Measurements.

Biophys Chem **1999**, *81* (1), 59–80. https://doi.org/https://doi.org/10.1016/S0301-4622(99)00082-4.

(38) Berry, J. D.; Neeson, M. J.; Dagastine, R. R.; Chan, D. Y. C.; Tabor, R. F. Measurement of Surface and Interfacial Tension Using Pendant Drop Tensiometry. *J Colloid Interface Sci* **2015**, *454*, 226–237. https://doi.org/https://doi.org/10.1016/j.jcis.2015.05.012.

(39) ASTM International. *Standard Practice for Exposure of Photodegradable Plastics in a Xenon Arc Apparatus*; 2021.

(40) Bharti, B.; Meissner, J.; Findenegg, G. H. Aggregation of Silica Nanoparticles Directed by Adsorption of Lysozyme. *Langmuir* **2011**, *27* (16), 9823–9833. https://doi.org/10.1021/la201898v.

(41) Annunziato, K. M.; Doherty, J.; Lee, J.; Clark, J. M.; Liang, W.; Clark, C. W.; Nguyen, M.; Roy, M. A.; Timme-Laragy, A. R. Chemical Characterization of a Legacy Aqueous Film-Forming Foam Sample and Developmental Toxicity in Zebrafish (Danio Rerio). *Environ Health Perspect* **2020**, *128* (9), 097006. https://doi.org/https://doi.org/10.1289/EHP6470.

(42) Moody, C. A.; Field, J. A. Perfluorinated Surfactants and the Environmental Implications of Their Use in Fire-Fighting Foams. *Environ Sci Technol* **2000**, *34* (18), 3864–3870. https://doi.org/10.1021/es991359u.

(43) Backe, W. J.; Day, T. C.; Field, J. A. Zwitterionic, Cationic, and Anionic Fluorinated Chemicals in Aqueous Film Forming Foam Formulations and Groundwater from U.S. Military Bases by Nonaqueous Large-Volume Injection HPLC-MS/MS. *Environ Sci Technol* **2013**, *47* (10), 5226–5234. https://doi.org/10.1021/es3034999.

(44) Adamson, D. T.; Kulkarni, P. R.; Nickerson, A.; Higgins, C. P.; Field, J.; Schwichtenberg, T.; Newell, C.; Kornuc, J. J. Characterization of Relevant Site-Specific PFAS Fate and Transport Processes at Multiple AFFF Sites. *Environmental Advances* **2022**, *7*, 100167. https://doi.org/https://doi.org/10.1016/j.envadv.2022.100167.

(45) Zhou, X.; Zhou, X. THE UNIT PROBLEM IN THE THERMODYNAMIC CALCULATION OF ADSORPTION USING THE LANGMUIR EQUATION. *Chem Eng Commun* **2014**, *201* (11), 1459–1467. https://doi.org/10.1080/00986445.2013.818541.

(46) Li, Z.; Gallus, L. Adsorption of Dodecyl Trimethylammonium and Hexadecyl Trimethylammonium onto Kaolinite — Competitive Adsorption and Chain Length Effect. *Appl Clay Sci* **2007**, *35* (3), 250–257. https://doi.org/https://doi.org/10.1016/j.clay.2006.09.004.

(47) Alves, A. V; Tsianou, M.; Alexandridis, P. Fluorinated Surfactant Adsorption on Mineral Surfaces: Implications for PFAS Fate and Transport in the Environment. *Surfaces*. 2020, pp 516–566. https://doi.org/10.3390/surfaces3040037.

(48) Kabiri, S.; Tucker, W.; Navarro, D. A.; Bräunig, J.; Thompson, K.; Knight, E. R.; Nguyen, T. M. H.; Grimison, C.; Barnes, C. M.; Higgins, C. P.; Mueller, J. F.; Kookana, R. S.;

McLaughlin, M. J. Comparing the Leaching Behavior of Per- and Polyfluoroalkyl Substances from Contaminated Soils Using Static and Column Leaching Tests. *Environ Sci Technol* **2022**, *56* (1), 368–378. https://doi.org/10.1021/acs.est.1c06604.

(49) Knutsen, H.; Mæhlum, T.; Haarstad, K.; Slinde, G. A.; Arp, H. P. H. Leachate Emissions of Short- and Long-Chain per- and Polyfluoralkyl Substances (PFASs) from Various Norwegian Landfills. *Environ Sci Process Impacts* **2019**, *21* (11), 1970–1979. https://doi.org/10.1039/C9EM00170K.

(50) Zhi, Y.; Lu, H.; Grieger, K. D.; Munoz, G.; Li, W.; Wang, X.; He, Q.; Qian, S. Bioaccumulation and Translocation of 6:2 Fluorotelomer Sulfonate, GenX, and Perfluoroalkyl Acids by Urban Spontaneous Plants. *ACS ES&T Engineering* **2022**, *2* (7), 1169–1178. https://doi.org/10.1021/acsestengg.1c00423.

(51) Wellen, B. A.; Lach, E. A.; Allen, H. C. Surface PKa of Octanoic, Nonanoic, and Decanoic Fatty Acids at the Air–Water Interface: Applications to Atmospheric Aerosol Chemistry. *Physical Chemistry Chemical Physics* **2017**, *19* (39), 26551–26558. https://doi.org/10.1039/C7CP04527A.

(52) Al Harraq, A.; Brahana, P. J.; Arcemont, O.; Zhang, D.; Valsaraj, K. T.; Bharti, B. Effects of Weathering on Microplastic Dispersibility and Pollutant Uptake Capacity. *ACS Environmental Au* **2022**. https://doi.org/10.1021/acsenvironau.2c00036.

(53) Chen, W.; Zhang, X.; Mamadiev, M.; Wang, Z. Sorption of Perfluorooctane Sulfonate and Perfluorooctanoate on Polyacrylonitrile Fiber-Derived Activated Carbon Fibers: In Comparison with Activated Carbon. *RSC Adv.* **2017**, *7*, 927–938. https://doi.org/10.1039/C6RA25230C.

(54) Gao, X.; Chorover, J. Adsorption of Perfluorooctanoic Acid and Perfluorooctanesulfonic Acid to Iron Oxide Surfaces as Studied by Flow-through ATR-FTIR Spectroscopy. *Environmental Chemistry* **2012**, *9*, 148. https://doi.org/10.1071/EN11119.

(55) Ward, R. N.; Davies, P. B.; Bain, C. D. Orientation of Surfactants Adsorbed on a Hydrophobic Surface. *Journal of Physical Chemistry* **1993**, *97* (28), 7141–7143. https://doi.org/10.1021/j100130a005.

(56) Schneider, C. A.; Rasband, W. S.; Eliceiri, K. W. NIH Image to ImageJ: 25 Years of Image Analysis. *Nat Methods* **2012**, *9* (7), 671–675. https://doi.org/10.1038/nmeth.2089.

(57) Trozzolo, A. M.; Winslow, F. H. A Mechanism for the Oxidative Photodegradation of Polyethylene. *Macromolecules* **1968**, *1* (1), 98–100. https://doi.org/10.1021/ma60001a019.

(58) TenCate Geosynthetics. *UV Durability of Tencate Geosynthetics*. https://www.tencategeo.us/media/40880ad4-a3aa-4ccc-b7f8-7697799698a4/PhH-Hg/TenCate Geosynthetics/Documents AMER/Technical Notes/General Technical Notes/TN_UV0419.pdf.

(59) Chen, H.; Reinhard, M.; Nguyen, V. T.; Gin, K. Y. H. Reversible and Irreversible Sorption of Perfluorinated Compounds (PFCs) by Sediments of an Urban Reservoir. *Chemosphere* **2016**, *144*, 1747–1753. https://doi.org/10.1016/j.chemosphere.2015.10.055.

(60) Meyers, D. Surfactants at the Solid Liquid Interface. In *Surfactant Science and Technology*; VCH Publishers: New York, New York, 1946; pp 300–301.

(61) Hunter, R. J. *Foundations of Colloid Science*, 2nd ed.; Oxford University Press: New York, 2001.

(62) Xue, X.; Hong, S.; Cheng, R.; Li, H.; Qiu, L.; Fang, C. Adsorption Characteristics of Antibiotics on Microplastics: The Effect of Surface Contamination with an Anionic Surfactant. *Chemosphere* **2022**, *307*, 136195. https://doi.org/https://doi.org/10.1016/j.chemosphere.2022.136195.

(63) Shen, M.; Song, B.; Zeng, G.; Zhang, Y.; Teng, F.; Zhou, C. Surfactant Changes Lead Adsorption Behaviors and Mechanisms on Microplastics. *Chemical Engineering Journal* **2021**, *405*, 126989. https://doi.org/https://doi.org/10.1016/j.cej.2020.126989.

(64) Xia, Y.; Zhou, J.-J.; Gong, Y.-Y.; Li, Z.-J.; Zeng, E. Y. Strong Influence of Surfactants on Virgin Hydrophobic Microplastics Adsorbing Ionic Organic Pollutants. *Environmental Pollution* **2020**, *265*, 115061. https://doi.org/https://doi.org/10.1016/j.envpol.2020.115061.

(65) Gao, Y.; Le, S.-T.; Kibbey, T. C. G.; Glamore, W.; O'Carroll, D. M. A Fundamental Model for Calculating Interfacial Adsorption of Complex Ionic and Nonionic PFAS Mixtures in the Presence of Mixed Salts. *Environ Sci Process Impacts* **2023**. https://doi.org/10.1039/D2EM00466F.

(66) Sharma, K. P.; Aswal, V. K.; Kumaraswamy, G. Adsorption of Nonionic Surfactant on Silica Nanoparticles: Structure and Resultant Interparticle Interactions. *J Phys Chem B* **2010**, *114* (34), 10986–10994. https://doi.org/10.1021/jp1033799.

(67) Borglin, S.; Shore, J.; Worden, H.; Jain, R. An Overview of the Sustainability of Solid Waste Management at Military Installations. *International Journal of Environmental Technology and Management* **2010**, *13* (1), 51–83.